

Spectral density for a hole in an antiferromagnetic stripe phase

P. Wróbel¹ and R. Eder²

¹ *Institute for Low Temperature and Structure Research, P. O. Box 1410, 50-950 Wrocław 2, Poland*

² *Institut für Theoretische Physik, Universität = Würzburg, Am Hubland, 97074 Würzburg, Germany*
(November 21, 2018)

Using variational trial wave function based on the string picture we study the motion of a single mobile hole in the stripe phase of the doped antiferromagnet. The holes within the stripes are taken to be = static, the undoped antiferromagnetic domains in between the hole stripes are assumed to have alternating staggered magnetization, as is suggested = by neutron scattering experiments. The system is described by the $t - t' - t'' - J$ model with realistic parameters and we compute the single particle spectral density.

PACS numbers: 71.27.+a, 74.20.Mn, 75.25.+z, 79.60.-i

I. INTRODUCTION

The experimental discovery of static stripe-like structures in some cuprate materials and nickelates¹ has recently attracted considerable attention. This is particularly remarkable for the cuprate superconductors because stripe-like hole arrangements have been predicted long ago by Hartree-Fock calculations for the d - p model² as well as for the single-band Hubbard model³ - these would then in some sense be the first successful theoretical predictions ever made for these materials. So far, there appears to be experimental evidence for stripes in a CuO_2 based material only for the concentration of $x = 3D1/8$, where the material does not superconduct. This might suggest that the stripes in this case are a kind of CDW-instability, stabilized predominantly by Coulomb interaction between holes, which occurs only at this special concentration. On the other hand, the rather precise scaling of the vector of magnetic incommensurability in $\text{La}_{2-x}\text{Sr}_x\text{CuO}_4$ with x for hole concentrations $x \leq 15\%$ can be quite naturally explained by assuming that fluctuating stripes with an x -independent hole density of $1/2$ within the stripes and a mean spacing of $\approx 1/2x$ between stripes do exist, which are separated by Néel ordered domains with alternating staggered magnetization.

In that sense, stripes could be a generic feature of a doped Heisenberg antiferromagnet. Exact diagonalization (ED) studies of the t - J model have shown evidence for stripe-like hole correlations in the ground state⁴, as well as low-energy excited states where the holes form stripe-like arrangements⁵. These results cannot actually be compared to the experimental situation, because the relatively small size of clusters available for the ED technique does not allow to accommodate a sufficiently large supercell as is observed experimentally. This is possible, however, in density matrix renormalization group calculations and this technique also has produced strong evidence⁶ for stripe-like hole arrangements in the ground state, or at least in very low excited states of the t - J model.

In the present paper we do not want to address the ques-

tion whether stripes really do form in the t - J model or what is the energy responsible for their stabilization. Instead, we take the existence of a stripe-like hole arrangement for granted, and study the dispersion and spectral function of an additional hole, which is moving through the stripe ‘background’. In other words: we want to discuss the photoemission spectrum of a striped phase. This seems an interesting question, because recently angle resolved photoemission (ARPES) data for $\text{La}_{2-x}\text{Sr}_x\text{CuO}_4$ have become available⁷. This compound is known to show stripe order for $x = 3D1/8$ and the ARPES spectra show a rather nontrivial evolution from the hole dispersion in the insulator ($x = 3D0$) which is very similar to $\text{Sr}_2\text{CuO}_2\text{Cl}_2$ ⁸, via the formation of ‘new states’ near $(\pi, 0)$ or $(0, \pi)$ to a very different spectrum for the superconducting phase ($x \approx 0.15$). Our intention is to check whether this can be reproduced by studying, in much the same way as the hole motion in an antiferromagnet is being studied, the motion of a single mobile hole in a static background of spins and immobile holes, shown in Figure 1, which form a stripe pattern rather than the conventional undoped Néel state.

We used the t - J Hamiltonian:

$$H = 3D - \sum_{i,j} \left(t_{ij} \hat{c}_{i,\sigma}^\dagger \hat{c}_{j,\sigma} + H.c. \right) + J \sum_{\langle i,j \rangle} \left(\vec{S}_i \cdot \vec{S}_j - \frac{\hat{n}_i \hat{n}_j}{4} \right). \quad (1)$$

Here $\hat{c}_{i,\sigma}^\dagger = 3D c_{i,\sigma}^\dagger (1 - n_{i,\bar{\sigma}})$ are the standard conditional electron creation operators, which avoid double occupancies, \vec{S}_i the operators of electron spin, and \hat{n}_i occupation numbers. The hopping integral t_{ij} between nearest neighbors was taken to be $t = 3D1$, that for 2^{nd} nearest neighbors was taken as $t' = 3D - 0.3$, the one between 3^{rd} nearest neighbors was $t'' = 3D0.3$. All other hopping integrals, as well as all exchange constants for other than nearest neighbors were taken to be zero. The nearest neighbor exchange constant was $J = 3D0.4$.

The hole motion in an antiferromagnet can be understood at least qualitatively within the string picture^{9,10}.

A hole created in a Néel state cannot propagate, because it leaves behind a trace of misaligned spins. This means that the magnetic frustration in the system increases to good approximation linearly with the distance travelled by the hole, whence the hole experiences an ‘effective potential’ which traps it around the site where it has been created. The wave function of the respective self-trapped state can be obtained by diagonalizing the Hamiltonian in the subspace of ‘string states’ where the hole is connected to its starting point i by strings of defects with various length and topology. True delocalization then is possibly only by virtue of the transverse part of the Heisenberg exchange which can ‘heal’ the defects created by the hopping hole. In fact, if the first two defects created by the hole are repaired by the transverse exchange, this amounts to shifting the starting point of the string to a 2^{nd} or 3^{rd} nearest neighbor of i . The resulting next-nearest neighbor hopping band of width $\propto J$ is indeed well established by a variety of techniques, both numerically and analytically¹¹. One may expect quite similar processes to occur also in a stripe-like background such as the one shown in Figure 1. The holes in the stripes thereby are to be considered as static. Also in this case an added mobile hole cannot propagate freely, because it creates frustration in the remaining antiferromagnetic volume of the system. Again the spin-flip parts will be necessary to enable propagation across the = antiferromagnetic stripes. The main difference then is that there may be additional processes when the hole passes through the hole stripes, and the fact that these hole stripes form something like ‘ $\lambda/2$ -plates’ for the propagating hole, because they separate antiferromagnetic domains with opposite staggered magnetization. As already mentioned the latter property is an experimental constraint, which is necessary to explain the incommensurate low energy peaks in neutron scattering. The calculation for the stripe background thus will be somewhat more complicated than for the case of the pure Néel state, but in principle the formalism is precisely the same. In the following we outline the respective calculation and present the results. As will be seen below, the computed single-particle spectra show some resemblance with the experimental results of Ino *et al.*

II. SPIN POLARONS IN THE STRIPE STRUCTURE

Our goal is to discuss the motion of holes in the stripe structure shown in Figure 1. In the following, we denote this state as $|\Phi_0\rangle$. It corresponds to a concentration of static holes of $1/8 = 3D12.5\%$ and has been suggested by experiments¹. The 32 sites contained in the rectangle in Fig.1 form the unit cell of this structure. Some theoretical studies suggest different structures⁶ but also indicate a tendency towards formation of stripes. Charge or spin order within the stripes has not actually been observed.

The pattern depicted in Fig.1 has been chosen for simplicity. The charge and spin fluctuations within stripes might, in principle, be taken into account in subsequent steps of approximation, but here we restrict ourselves to the simplest case possible, namely static holes and spins. We stress again that our aim is not to discuss the stability of the stripe structure, but rather to take it for granted, and concentrate on the properties of an additional hole injected into the stripe structure. We assume that its dynamics is represented by the standard $t - J$ model, augmented by additional next-nearest neighbor (t') and next-next-nearest (t'') hopping terms. Such terms are necessary¹²⁻¹⁶ to explain the dispersion in the insulating CuO₂ plane as measured by Wells *et al.*⁸.

As already mentioned, a mobile hole which has been created in an ideal antiferromagnetic background behaves as if it is trapped in a kind of potential well⁹. The reason is that its movement creates strings of misaligned spins in the antiferromagnetic structure and thus increases the magnetic energy. These strings of defects, tend to restrict the motion of the hole to the neighborhood of the site where it has been created. The notion of this effective potential well for the hole is equivalent to the idea of ‘spin bags’ which was introduced in the context of the Hubbard model¹⁷. Coherent motion of holes is possible due to relaxation of strings which is enabled predominantly by the transverse part of the Heisenberg exchange contained in the $t - J$ model. The motion of a hole, then, has a twofold character. Because of $t > J, t, t', t''$, the hole will oscillate rapidly (with a hopping rate $\propto t^{-1}$) in the neighborhood of the site to which it is attached by the string and only rarely (at a rate $\propto J^{-1}$) the exchange part will shorten the string of defects by two. This means that the starting point of the string, and hence the center of gravity of the oscillatory motion, is shifted by two lattice spacings.

In order to describe this twofold dynamics of holes we first construct wave functions which describe a self-trapped state of the hole. We first introduce the operators

$$T_{\langle i,j \rangle} = 3D \left(c_{i,\downarrow}^\dagger c_{j,\downarrow} + c_{j,\uparrow}^\dagger c_{i,\uparrow} \right). \quad (2)$$

In an arbitrary spin background they shift holes by one lattice spacing. By consecutively applying the $T_{\langle i,j \rangle}$ to a the state $\hat{c}_l |\Phi_0\rangle$, we generate a family of string states. The strings of defects connect the hole to the site l . We denote such a string state by $|l, \mathcal{P}_l\rangle$, whereby \mathcal{P}_l stands for a set of numbers which give the topology of the string. We will choose $\mathcal{P} = 3D(\mathbf{e}_1, \mathbf{e}_2, \dots)$, where the unit vector $\mathbf{e}_i \in \{\pm \mathbf{e}_x, \pm \mathbf{e}_y\}$ gives the direction of the i^{th} hop which the hole has taken. For the wave function of a hole trapped in the vicinity of the site l we then make the ansatz:

$$|\Psi_l\rangle = 3D \sum_{\{\mathcal{P}_l\}} \alpha_{l, \mathcal{P}_l} |l, \mathcal{P}_l\rangle. \quad (3)$$

For the Hamiltonian we choose the sum of the kinetic energy and Ising part of the Heisenberg exchange:

$$H_0 = 3D - t \sum_{\langle i,j \rangle} \sum_{\sigma} (\hat{c}_{i,\sigma}^{\dagger} \hat{c}_{j,\sigma} + H.c.) + J \sum_{\langle i,j \rangle} \left(S_i^z S_j^z - \frac{\hat{n}_i \hat{n}_j}{4} \right) \quad (4)$$

The kinetic energy has matrix elements of $-t$ between two states $|l, \mathcal{P}_l\rangle$ and $|l, \mathcal{P}'_l\rangle$ if the respective paths can be transformed into each other by a single hop. The diagonal matrix elements of H_0 originate from the term $J \sum_{\langle i,j \rangle} (S_{i,z} S_{j,z} - n_i n_j / 4)$. If we choose the state $|\Phi_0\rangle$ as the zero of energy for these diagonal matrix elements, the energy of any given string state is simply the number of additional ‘broken’ bonds times $J/2$. For example the energy of the state $\hat{c}_{(0,1),\uparrow} |\Phi_0\rangle$ is $J/2$, while for the state $\hat{c}_{(-1,1),\uparrow} |\Phi_0\rangle$ it is $3J/2$.

Once we truncate the subspace of string states (for example by taking into account only paths up to a maximum length) we can easily set up the matrix corresponding to H_0 and diagonalize it numerically to obtain the ground state

$$H_0 |\Psi_l\rangle = 3DE_l |\Psi_l\rangle. \quad (5)$$

This gives us the coefficients α_{l,\mathcal{P}_l} in (3) as well as the (l -dependent) ground state energy E_l . This procedure can be performed for any ‘environment’ which the hole has been created in. The variation of the wave function $|\Psi_l\rangle$ with l describes how the spin bag is ‘deformed’ by its local environment. This ‘prediagonalization’ of H_0 reduces the number of degrees of freedom considerably, and thus makes the problem tractable even with the relatively large unit-cell for the stripe structure. This is also the main difference compared to the related method of Trugman¹⁰, which obtains the ground state wave function by constructing one Bloch states from each of the string states $|l, \mathcal{P}\rangle$. Neglecting the excited states of H_0 in the further steps of the calculation is justified provided the separation in energy between these excited states and the ground state is sufficiently large so that transitions into these states can be neglected. We have verified that the separation in energy between the ground state and the first excited state is in any case $\geq J/2$, in most cases even larger than J . Since the bandwidth for a single hole is $\approx 2J$, neglecting these excited states is probably not really an excellent but reasonable approximation.

In our calculation we have used the part of the Hilbert space defined by the condition $S_z = 3D - 1/2$, where S_z is the z component of the total spin. The other possible choice $S_z = 3D + 1/2$ would give identical results, corresponding to a hole moving on the opposite sublattice. The condition $S_z = 3D - 1/2$ may be fulfilled by removing an up spin from the stripe structure. There are 14 non-equivalent spin-up sites in the elementary cell in Figure 1. The presence of the ferromagnetic bonds across the stripes brings about an extra complication:

some of states that represent holes created in stripes are directly coupled by the ‘fast’ nearest neighbor hopping term. For example, the state $\hat{c}_{(5,1),\uparrow} |\Phi_0\rangle$ may be obtained by acting only once with the operator T_{\dots} on $\hat{c}_{(4,1),\uparrow} |\Phi_0\rangle$. This cannot happen in the Néel state, where sites of like spin are always separated by at least 2 lattice spacings, and thus are not coupled by one nearest neighbor hop. To deal with this situation, we incorporate both states, $\hat{c}_{(5,1),\uparrow} |\Phi_0\rangle$ and $\hat{c}_{(4,1),\uparrow} |\Phi_0\rangle$, into one and the same self-trapped state $|\Psi_l\rangle$, which consequently is elongated in x -direction. In this way the number of non-equivalent starting points l for holes is reduced to the following 12 sites: (0, 1), (1, 0), (1, 2), (2, 1), (2, 3), (3, 0), (3, 2), (4, 1), (5, 3), (6, 0), (6, 2) and (7, 3). Finally, it turns out that some starting points l for holes are equivalent in that the respective spin polaron states $|\Psi_l\rangle$ may be transformed into one other by applying a symmetry transformation of the stripe structure. For example, the sites (0, 1) and (4, 1) which belong to the same elementary cell are equivalent.

By means of computer algebra we can now create the states $|\Psi_l\rangle$. The algorithm thereby takes into account exactly strings of length up to 3 lattice spacings. For longer paths (which are less relevant) the approximation is made that their amplitude in $|\Psi_l\rangle$ does not depend on details of further steps. At this stage of the calculation we also make the assumption that the states $|l, \mathcal{P}_l\rangle$ for different l and/or different \mathcal{P}_l are always orthogonal. For longer paths this may not be true. The stripe pattern provides much more possibilities to reach identical states from different original configurations, not only by means of retracing paths as it is basically in the case of the Néel state, but we neglect this here. As already mentioned, any charge and spin fluctuations of the holes and spins which form the background stripe pattern are also neglected.

It then turns out that the differences between the eigenenergies E_l of spin-polaron states for different initial positions l of the hole are $\sim J$. The states which are lowest in energy thereby correspond to polarons centered on (0, 1), (4, 1) and equivalent positions. We see that despite the fact that the freedom of motion of a hole created at the site (0, 1) is strongly reduced by the (static) holes at (0, 0) and (0, 2), which inevitably results in a loss of kinetic energy, there is a net gain in energy compared to other sites. This is obviously due to the smaller number of broken bonds created in the first few hops. This means first of all a lower exchange energy, and second a gain in kinetic energy because the hole can move more freely along the remaining paths. We do not pursue this any further, but we note that this may be one reason for the stability of stripes.

III. PROPAGATION OF SPIN POLARONS IN THE STRIPE STRUCTURE

So far we have constructed wave function for self-trapped states at various positions in the stripe structure. We now assume that the wave function for a hole added to the stripe structure is a coherent combination of these polaron states $|\Psi_l\rangle$. All processes which were neglected when constructing the self-trapped states $|\Psi_l\rangle$ will now be incorporated into an effective Hamiltonian H_{eff} which couples the $|\Psi_l\rangle$ centered on different l . As already mentioned, in doing so we implicitly assume that the excited states which come out of (3) are separated from the ground state by an energy which significantly exceeds the matrix elements of H_{eff} .

The diagonal element $\langle\Psi_l|H_{eff}|\Psi_l\rangle$ is essentially the eigenenergy E_l of the polaron-state $|\Psi_l\rangle$. It influences the probability that a particular site is occupied by the polaron. By means of computer algebra we have also set up additional diagonal and off-diagonal contributions to H_{eff} . Thereby we have confined the search to paths no longer than 2 lattice spacings. There are several hundreds of process which couple pairs of sites one of which (at least) belongs to the elementary cell. They form 29 different categories of processes. We shall now discuss some examples.

To begin with, the possibility of direct hopping to second nearest neighbors by virtue of the t' -term in the $t-J$ model has not been taken into account when setting up the different H_0 . Therefore, H_{eff} must take it into account. Consider Fig.2. Shifting a hole created at the site (0,1) by (1,1) gives rise to a state that represents a hole created at (1,2). This process therefore couples the states $|\Psi_{(0,1)}\rangle$ and $|\Psi_{(1,2)}\rangle$, the numerical value of the corresponding matrix element $\langle\Psi_{(0,1)}|H_{eff}|\Psi_{(1,2)}\rangle$ is $t'\alpha_{(0,1)}\alpha_{(1,2)}$. Here pairs of numbers in subscripts refer to position of holes, and the α 's are obtained by diagonalizing the H_0 matrices.

Next, Fig.2(a,b,c) depicts a process which contributes to the diagonal element for the spin-polaron state at (2,1). After a single hop in the (1,0) direction a hole created at (2,1) occupies the site (3,1). The amplitude of this state in $|\Psi_{(2,1)}\rangle$ is $\alpha_{l,\mathcal{P}_l} = 3D\alpha_{(2,1),(1,0)}$, where, as explained above, the first pair of numbers denotes the original position of the hole whereas the second pair gives the direction of the hop. Next, let us assume that the t' term now shifts the hole to the site (2,2). This state has the coefficient $\alpha_{(2,1),(0,1)}$ in $|\Psi_{(2,1)}\rangle$ whence we have found a contribution of $t'\alpha_{(2,1),(1,0)}\alpha_{(2,1),(0,1)}$ to the matrix element $\langle\Psi_{(2,1)}|H_{eff}|\Psi_{(2,1)}\rangle$.

There are a few more types of processes that involve the t' term. In Fig.2(d) we start with the string state obtained by creating a hole at (2,3) and performing two hops in directions (1,0) and (0,1). Shifting the hole in $(-1,-1)$ direction by virtue of t' , this is transformed into a state obtained by creating a hole at (3,4) and shifting it in the directions (0,-1) and $(-1,0)$ (Fig.2(e)). This type of

process couples polarons at the sites (2,3) and (3,4) and the corresponding contribution to $\langle\Psi_{(2,3)}|H_{eff}|\Psi_{(3,4)}\rangle$ is $t'\alpha_{(2,3),(1,0)}\alpha_{(3,0),(0,-1)}\alpha_{(-1,0)}$. Yet another process is possible due to the existence of parallel spins on nearest neighbor sites in the stripe structure. Shifting a hole created at the site (3,2) (see Fig.2(f)) by (1,1) produces the same state as obtained = by two hops of this hole in the directions (0,1) and (1,0). The corresponding contribution to the matrix element $\langle\Psi_{(3,2)}|H_{eff}|\Psi_{(3,2)}\rangle$ is $t'\alpha_{(3,2)}\alpha_{(3,2),(0,1)}\alpha_{(1,0)}$.

The third nearest neighbor hopping term t'' model gives rise to similar additions to H_{eff} . For example a contribution $t''\alpha_{(5,3)}\alpha_{(7,3)}$ to $\langle\Psi_{(5,3)}|H_{eff}|\Psi_{(7,3)}\rangle$ emerges due to the possibility of direct hopping = of a hole from (5,3) \rightarrow (7,3). Fig.3 shows a process whereby a hole created at the site (4,5) (Fig.3(a)) which hopped three times in the directions (1,0), (0,-1) and (0,-1) (Fig.3(b)) is shifted by (0,2). The resulting state (Fig.3(c)) then represents a hole created at (5,3) which hopped twice in direction (0,1). That gives rise to a contribution $-t''\alpha_{(4,5),(1,0)}\alpha_{(0,-1)}\alpha_{(0,-1)}\alpha_{(5,3),(0,1)}\alpha_{(0,1)}$ to the matrix element $\langle\Psi_{(4,5)}|H_{eff}|\Psi_{(5,3)}\rangle$. The minus sign stems from Fermi statistics and the definition of the operator $T_{(i,j)}$ which creates string states and the fact that the length of the first string is odd, while the length of the second is even.

This concludes our discussion of the effects of t' and t'' and we now proceed to a discussion of contributions to H_{eff} which originate from the exchange part of the $t-J$ model. Fig.4(a,b,c,d) depicts a process that involves pairs of parallel spins on nearest neighbor sites in the stripe structure. Fig.4(a,b) shows holes which have been created at the sites (4,1) and (8,1). After three hops in the direction $(-1,0)$ the hole from the site (8,1) reaches the site (5,1). Fig.4(c) shows the corresponding string state which is a component of the spin polaron at the site (8,1). By acting with the spin-flip term on the bond (6,1)-(7,1) this state is transformed into the state in Fig.4(d), which in turn is a string state which is a component of the spin polaron at the site (4,1). To be more precise, the state in Fig.4(d) can be obtained by a single hop in the (1,0) direction from the state in Fig.4a. The matrix element describing the process in Fig.4(a,b,c,d) is $(J/2)\alpha_{(4,1),(1,0)}\alpha_{(8,1),(-1,0)}\alpha_{(-1,0)}\alpha_{(-1,0)}$. This mechanism of coupling spin polarons at the sites (4,1) and (8,1) also works for all longer string states where the hole in Fig.4(c) and (d) has moved in the vertical direction. This motion does not interfere with the action of the exchange term on the sites (6,1) and (7,1) which gives rise to the equivalence of string states formed by further motion of the hole in Fig.4(c) and (d). The above contribution to H_{eff} therefore should be supplemented by terms related to all relevant longer paths.

Quite generally it is obvious that Figures 2,3, and 4 represent only a small fraction of all processes which may occur during the motion of a hole through the stripe background. There are various inequivalent positions of polarons within the unit cell and the different local ar-

rangement of spins and holes in the stripes gives rise to many non-equivalent processes which however may be easily found by means of computer algebra.

As we have mentioned before, spin and charge fluctuations have been neglected in our calculation. They influence to some extent the = properties of the system. Nevertheless, it seems plausible as a first attempt to treat the stripe structure as a static object and discuss the = propagation of an excess hole in the stripe background. We expect to gain in this way some insight into electronic properties of stripes.

In order to construct a coherent combination of spin polaron states we have to label the positions of polarons in a slightly different way. = We identify a site l by the vector \mathbf{R}_m which gives the position of the lower left corner of the elementary cell containing the site and the position n of the site within the elementary cell:

$$|\Psi_l\rangle \equiv |\Psi_{\mathbf{R}_m, n}\rangle \quad (6)$$

A Bloch state $|\tilde{\Psi}\rangle$ with momentum \mathbf{P} then can be written as

$$|\tilde{\Psi}_n\rangle = 3D \frac{1}{\sqrt{N'}} e^{i\mathbf{R}_m \mathbf{P}} \sum_m |\Psi_{\mathbf{R}_m, n}\rangle, \quad (7)$$

where N' is a normalization constant, i.e. the number of elementary cells in a system with periodic boundary conditions. The momentum \mathbf{P} has to be chosen from the reduced Brillouin zone $[-\frac{\pi}{8}, \frac{\pi}{8}] \otimes [-\frac{\pi}{4}, \frac{\pi}{4}]$. The states $|\tilde{\Psi}_n\rangle$ are normalized by definition:

$$\langle \tilde{\Psi}_n | \tilde{\Psi}_{n'} \rangle = 3D \delta_{n, n'} \quad (8)$$

The states $|\tilde{\Psi}_{n'}\rangle$ and $|\tilde{\Psi}_n\rangle$ for different sites n and n' in the elementary cell are orthogonal because up to the accuracy level of our calculation different string states are orthogonal. The matrix elements of the Hamiltonian for the coherent combinations $|\tilde{\Psi}_n\rangle =$ then may be represented in terms of the matrix elements for spin polarons which we already know:

$$\langle \tilde{\Psi}_n | H_{eff} | \tilde{\Psi}_{n'} \rangle = 3D \sum_{m'} e^{i\mathbf{R}_{m'} \mathbf{P}} \langle \Psi_{0, n} | H_{eff} | \Psi_{\mathbf{R}_{m'}, n'} \rangle. \quad (9)$$

In order to get a feeling for the evolution with doping we have analyzed an analogous stripe structure, shown in Figure 5, which would correspond to the case of 1 hole per 12 copper sites. The existence of stripes at this level of doping is as yet a speculation. Stripes, if they exist at all, may in this case have a dynamical character. Nevertheless, we have decided to use a structure which is analogous to the pattern that we used for the 1/8 case. This can also give some indication as to how robust the various features in the calculated spectral density are against possible changes of the structure. Finally, to conclude the discussion of the propagation of the mobile hole, we note that the dispersion relation for a hole

in the original Néel state, can be carried out in precisely the same way¹⁸. We have also performed this calculation to compare the dispersion for the Néel state and the stripe phase.

IV. SPECTRAL FUNCTION

We now proceed to discuss the one-particle spectral function and consider the term related to creation of an additional hole in the stripe structure. It can be written as

$$A_h(\mathbf{k}, \omega) = 3D \sum_{\nu} |\langle \Phi_{\nu}^{(+1h)} | c_{\mathbf{k}, \uparrow} | \Phi_0 \rangle|^2 \delta \left(\omega - (E_{\nu}^{(+1h)} - E_0^{(s)}) \right), \quad (10)$$

where $|\Phi_{\nu}^{(+1h)}\rangle$ is an eigenstate corresponding to an additional hole inserted into the stripe structure and in our calculation is identified with the solution of the eigenvector problem for the Hamiltonian (9). The $c_{\mathbf{k}, \uparrow}$ operator may be written as

$$c_{\mathbf{k}, \uparrow} = 3D \frac{1}{\sqrt{N}} \sum_n e^{-i\mathbf{k} \mathbf{R}_n} c_{n, \uparrow}. \quad (11)$$

The summation here runs over all sites in the lattice and $N = 3D32N'$ is their total number. The ν -th excited state $|\Phi_{\nu}^{(+1h)}\rangle$ is a linear combination of the states $|\tilde{\Psi}_n\rangle$:

$$|\Phi_{\nu}^{(+1h)}\rangle = 3D \sum_n \beta_{\nu}^{(n)} |\tilde{\Psi}_n\rangle. \quad (12)$$

The summation label n thereby refers to the 12 inequivalent sites in the elementary cell enumerated above, which may be occupied by a spin-up polaron. After some straightforward algebra = the relevant correlation function takes the simple form

$$\langle \Phi_{\nu}^{(+1h)} | c_{\mathbf{k}, \uparrow} | \Phi_0^{(s)} \rangle = 3D \delta_{Mod(P_x + k_x, 2\pi/8), 0} \times \delta_{Mod(P_y + k_y, 2\pi/4), 0} \sqrt{\frac{N'}{N}} \sum_{n, l} (\beta_{\nu}^{(n)})^* e^{-i\mathbf{k} \mathbf{R}_l} \langle \Psi_{0, n} | c_{l, \uparrow} | \Phi_0 \rangle. \quad (13)$$

The matrix elements $\langle \Psi_{0, n} | c_{l, \uparrow} | \Phi_0 \rangle$ give the overlap between the bare hole created in the stripe structure = at site l and the self-trapped state centered on site n . Since the electron annihilation operator cannot create any spin defects, it can only produce the 'string of length zero'. Hence only the state $c_{n, \uparrow} | \Phi_0 \rangle$, which has the prefactor α_n in $|\Psi_{0, n}\rangle$, can possibly have a nonvanishing overlap with $c_{l, \uparrow} | \Phi_0 \rangle$. Therefore we have $\langle \Psi_{0, n} | c_{l, \uparrow} | \Phi_0 \rangle = 3D \delta_{l, n} \alpha_n$. The only exception are the 'elongated' states along the ferromagnetic bonds. As was explained above, the states obtained by creating a hole either at (4, 1) or at (5, 1) are both included into the self-trapped state centered on (4, 1). Hence

$$\langle \Psi_{(4,1),0} | c_{l,\uparrow} | \Phi_0 \rangle = 3D \delta_{l,(4,1)} \alpha_{(4,1)} - \delta_{l,(5,1)} \alpha_{(4,1),(1,0)}, \quad (14)$$

where the relative minus between the two contributions is due to Fermi statistics.

We have employed the formula (13), together with the above expressions for the matrix elements, in the evaluation of the spectral functions. It should be noted that the resulting ‘spectral weight’ basically is a measure as to how well the respective many-body wave function matches the wave function of a photoelectron, which we model by a plane wave with momentum \mathbf{k} . The actual spectral weight observed in an angle resolved photoemission experiment may still differ from this: the spectral weight of a quasiparticle in the t-J model is known to have a significant \mathbf{k} dependence due to the quantum spin fluctuations of the Heisenberg antiferromagnet¹⁹, in the more realistic single²⁰ or three-band²¹ Hubbard model an additional \mathbf{k} dependence is brought about by charge fluctuations and/or interference between photoholes created on Cu and O sites²¹. Unfortunately these effects are beyond the scope of our approximation.

On the other hand, the Brillouin zone of the supercell in Figure 1 is $[-\frac{\pi}{8}, \frac{\pi}{8}] \otimes [-\frac{\pi}{4}, \frac{\pi}{4}]$. An angle resolved photoemission experiment with a momentum transfer of, for example, $\mathbf{k} = 3D(\pi, 0)$ thus actually probes the eigenvalue spectrum at $(\frac{\pi}{8}, 0)$. Any ‘dispersion’ which is measured on scales in \mathbf{k} space larger than the extent of the reduced Brillouin zone therefore is in reality a ‘spectral weight dispersion’ and cannot be interpreted as a band dispersion. This ‘dispersion’ then is essentially determined by the expression above, namely how well a photoelectron with the respective momentum matches the wave function of the respective state within the 32-site unit cell. In that sense the above ‘spectral weight’ does very well have some significance. Therefore, one may expect that although the magnitude of the spectral weight obtained from (13) cannot be directly compared to experiments, it still may give us a rough feeling as to where in (\mathbf{k}, ω) space we may expect nonvanishing weight.

The smallness of the reduced Brillouin zone brings about another complication: suppose we compute (as is usually done) the spectral function at an equally spaced \mathbf{k} -grid along some high-symmetry line, e.g. $(0, 0) \rightarrow (\pi, 0)$. Then, there are two possibilities: the step size of the \mathbf{k} -grid may be commensurate with the size of the reduced Brillouin zone or not. To illustrate the first case, let us assume the step size to be $\pi/8$. Then, we would actually be probing just two momenta in the reduced zone, namely $(\pi/8, 0)$ and $(0, 0)$. This would therefore give us an artificial periodicity of the peak positions (although not of the spectral weight). On the other hand, if we choose an incommensurate step size (we choose $\pi/7$ as an example) we would walk through the reduced Brillouin zone like this: $(0, 0), (-\frac{6\pi}{56}, 0), (\frac{2\pi}{56}, 0), (-\frac{4\pi}{56}, 0), (\frac{4\pi}{56}, 0) \dots$ that means more or less in a random sequence. Plotting the results for the spectral density in this way therefore is probably of very little significance. We have therefore

decided to average the spectra for each momentum over a small neighborhood of the respective momentum and compute:

$$\bar{A}(\mathbf{k}, \omega) = 3D \sum_{i,j} w_{i,j} A_h(\mathbf{k} + i\delta_x + j\delta_y, \omega). \quad (15)$$

We have chosen the weight function $w_{i,j}$ to be a constant and used $\delta_{x,y} = 3D \frac{\pi}{8 \cdot 16} \mathbf{e}_{x,y}$, and summed over $-8 \leq i, j \leq 8$. To some degree this also simulates the effect of the finite \mathbf{k} -resolution in an ARPES spectrum. Bearing this in mind we turn to the numerical results for the spectral density. Figures 6-10 then show the spectral function $\bar{A}(\mathbf{k}, \omega)$ calculated along various high-symmetry lines in the *extended* Brillouin zone. Distances in the k space between points in the sequence are equal. An important point for comparison with experiment is the following: we are using a hole language, which implies that the ground state of the hole is the state with the most negative energy. In a photoemission experiment the single-hole ground state then would actually be the first ionization state, i.e. the state with the lowest binding energy, and would form the ‘top of the band’. For comparison with the usual way of plotting experimental ARPES data, with binding energy increasing to the left, the energy axis in our figures would have to be inverted. To begin with, the direction $(0, 0) \rightarrow (\pi, \pi)$ (see Figure 10) and $(0, 0) \rightarrow (0, \pi)$ (which has momentum parallel to the stripes, see Figure 7) show a distribution of spectral weight which broadly follows the quasiparticle dispersion for the $t - t' - t'' - J$ model in the pure antiferromagnet (the latter is indicated by the full line). The direction $(\pi, 0) \rightarrow (\pi, \pi)$ (see Figure 8) might be interpreted as the superposition of two components, one of them following the antiferromagnetic quasiparticle dispersion, the other one forming a dispersionless band at $\approx -2.3t$. It should be noted, however, that in this part of the extended Brillouin zone the spectral weight of the quasiparticle band is practically zero in the antiferromagnet⁸, whence the dispersionless band is probably unobservable. The situation is different for the direction $(0, 0) \rightarrow (\pi, 0)$ (i.e. the momentum is perpendicular to the stripes), see Figure 6. In this direction we see several more or less dispersionless ‘bands’, and in particular a flat band of low energy states at $\approx -2.3t$. Since this range of momenta is within the antiferromagnetic Brillouin zone one may expect, based on the results for the antiferromagnet, that it has an appreciable spectral weight. A dispersionless band at $\approx -2.3t$ is also seen in the direction $(0, \pi) \rightarrow (\pi, \pi)$, but again thus is probably not observable because it is in the outer part of the extended Brillouin zone. Averaging the directions $(0, \pi)$ and $(\pi, 0)$, which presumably corresponds to the experimental situation because the stripes do not have a uniform direction throughout the sample, one would thus get a ‘broadened’ version of the quasiparticle band in the insulator, plus a relatively flat band of new states, which actually form the first ionization states. It is quite tempting to identify this with the experimental results of Ino *et*

al. At half-filling ($x = 3D0$), these data showed a dispersion which is very much reminiscent of the ‘quasiparticle band’ observed in $\text{Sr}_2\text{CuO}_2\text{Cl}_2$. As doping is increased, this band persists to some degree, although is getting more diffuse. In addition, around $(\pi, 0)$ a relatively dispersionless band of ‘new states’ emerges, which forms the first ionization states. In order to clarify the character of the wave functions, we have also studied the real space wave function $w_n = 3D|\beta_\nu^{(n)}|^2$ for different states (see Eq. (12)). This basically gives the probability to find the hole in the self-trapped state at site n within the unit cell. Figure 11 shows this for a state which produces an intense peak at $(\pi, 0)$, whereby the peak relatively far from the top of the band and thus would correspond to the ‘remnant of the antiferromagnetic band’. It is obvious from the figure, that the mobile hole in this case avoids the hole stripes and resides mainly in the center of one of the antiferromagnetic domains. On the other hand, Figure 12 shows the probability distribution for one of the ‘new states’ at $(\pi, 0)$. There the extra hole resides almost exclusively within the stripe. This shows again, that the new states, which appear upon doping, are related to states which are predominantly localized in the hole stripes. Of course one has to keep in mind that our approximation of static holes within the stripes will make the description of precisely these states the most questionable. Finally, Figure 13 shows w_n for a state which produces a significant peak at $(0, \pi)$ which also belongs to the ‘remnant of the antiferromagnetic band’. Again, we see that the mobile hole avoids the hole stripes, which is expected if the state somehow resembles properties of the undoped antiferromagnet. In order to understand the origin of some features observed in the spectra for the 1/8 case we have also performed the calculation of the spectral function for the structure represented by Fig. 5, which would correspond to the case of $\delta = 3D1/12$. Stripes at this level of doping, if exist, have a dynamical character and the applicability of the stiff structure represented by Fig. 5 is very questionable. Our aim was to check the robustness of some characteristics, rather than to derive any spectra comparable with experiments. Figures 14 and 15 depict spectra calculated along the lines $(0, 0) \rightarrow (\pi, 0)$ and $(0, 0) \rightarrow (\pi, \pi)$ respectively. We again notice a band at the energy $\approx -2.3t$ which emerges in the vicinity of $(\pi, 0)$ and disappears somewhere halfway to the point $(0, 0)$. We have checked that this band may be attributed to states that represent the extra hole which resides predominantly within the stripe. The rest of the spectrum seems to resemble the energy dispersion of a single hole in an antiferromagnet. We have not observed that for the 1/8 case when the size of antiferromagnetic domains is smaller. The states which form the ‘antiferromagnetic band’ correspond to the extra hole avoiding stripes. The spectrum for the direction $(0, 0) \rightarrow (\pi, \pi)$, however very broad, follows the quasiparticle dispersion of the pure antiferromagnet in a more evident way than for $\delta = 3D1/8$. These remarks in-

dicates that the evolution of the spectral function between doping levels $\delta = 3D0$ and $\delta = 3D1/8$ may be attributed to formation of stripes.

V. DISCUSSION

In summary, we have calculated the dispersion for a single mobile hole in a static stripe structure or, put another way, a depleted Heisenberg plane, thereby using a reasonably realistic version of the $t-t'-t''-J$ model. The strongest approximation presumably consisted in taking the holes in the stripes to be static, but we believe this is a reasonable first step in understanding the dynamics of holes in truly fluctuating stripes. In particular, the present calculation incorporates the effect of the oscillating direction of Néel order in the undoped antiferromagnetic domains of the stripe pattern, as well as the influence of the important t' and t'' terms on the hole motion. From the calculated dispersion and wave function we have computed the ‘spectral weight’ as a function of energy. This spectral weight is basically the overlap of the wave function in the supercell with a plane wave of the respective momentum. In an ARPES experiment on a system with a relatively small reduced Brillouin zone as the stripe structure with its large unit-cell, it is basically this ‘spectral weight dispersion’ which is being measured. As expected, the primary influence of the stripes is the ‘broadening’ of the spectral weight, which however still roughly follows the hole dispersion in the insulator, at least along some high-symmetry lines. This is to be expected for a not too strong super-cell potential. In addition, the stripes lead to the emerging of ‘new states’ near $(\pi, 0)$ at relatively low binding energy. More precisely, the spectral density in the stripe structure shows a rather sharp and dispersionless low energy band, which is presumably most intense around $(\pi, 0)$, and which actually forms the first ionization states. Analysis of the wave functions has shown, that the holes reside predominantly within the hole stripes in these new states, whereas the states responsible for the ‘remnants of the antiferromagnetic band’ in the spectral density have the holes predominantly in the antiferromagnetic domains. It is interesting to note that this effect, namely the generation of low energy states at $(\pi, 0)$ by going from the undoped to the doped system, can also be observed in exact diagonalization calculations for the $t-t'-t''-J$ model¹⁴. Whether this is due to formation of stripes even in the relatively small clusters studied remains to be clarified. In any case the effect of ‘doping’ (that means the modification of the Néel state to the stripe pattern with static holes and antiferromagnetic domains) on the spectral function in our calculation shows some similarity with recent ARPES measurements on $\text{La}_{2-x}\text{Sr}_x\text{CuO}_4$ ⁷. They covered the range from an optimally doped superconductor ($x = 3D0.15$) to an antiferromagnetic insulator ($x=3D0$). It has been suggested on the basis of the in-

commensurate peaks in inelastic neutron scattering^{1,22} that the family of LSCO systems reveals an instability towards a *static* spin-charge order of stripe form. The formation of these stripe structures is accompanied by a suppression of T_c at a hole concentration $\delta \simeq 1/8$. It should be noted that in the experimental ARPES spectra ‘peaks’ in the spectral density cannot usually be assigned. The various ‘bands’ in the spectra become visible only upon forming the 2nd derivative of the spectral density with respect to energy. For the insulating compound La_2CuO_4 the ‘dispersion’ roughly resembles the known band structure of a hole in an antiferromagnet as it has been observed in $\text{Sr}_2\text{CuO}_2\text{Cl}_2$: the top of the band appears to be at $(\pi/2, \pi/2)$, the band at $(\pi, 0)$ is at a significantly ($\approx 200\text{meV}$) higher binding energy. Upon doping this band structure of the insulator persists to some degree, but in addition ‘new states’ at $(\pi, 0)$ appear. These have a very low binding energy and indeed do form the first ionization states. Let us concentrate on the case of $x = 3D0.12$ which is closest to the configuration we have discussed. It is believed that stripe structures are perpendicular in nearest copper-oxygen planes. The spectra in the $(0, 0) \rightarrow (0, \pi)$ direction are a composition of spectra parallel and perpendicular to stripes. The measurements in that direction correspond rather well to a combination of our calculated spectra for the directions $(0, 0) \rightarrow (0, \pi)$ and $(0, 0) \rightarrow (\pi, 0)$. The same holds true for the direction $(\pi, 0) \rightarrow (\pi, \pi)$. Keeping that in mind we notice that the experimental and theoretical spectra show at least a qualitative agreement. In both cases we observe, along the directions $(0, 0) \rightarrow (\pi, 0)$ and $(0, 0) \rightarrow (0, \pi)$, the ‘splitting’ of the spectrum and formation of new low energy states around $(\pi, 0)$. This splitting is much less pronounced in the direction $(0, \pi) \rightarrow (\pi, \pi)$. The spectra along the direction $(\pi, 0) \rightarrow (\pi, \pi)$ are very broad. That prevents assignment of a band for some range of \mathbf{k} points in that direction. Finally, the spectra along the direction $(0, 0) \rightarrow (\pi, \pi)$ are very broad and it is practically impossible to distinguish any band.

Useful discussion with J. Zaanen are gratefully acknowledged. One of the authors (P.W.) acknowledges support by the Polish Science Committee (KBN) under contract No. 2PO3B-02415.

- ⁶ S. R. White and D. J. Scalapino, Phys. Rev. Lett. **80**, 1272 (1998); S. R. White and D. J. Scalapino, Phys. Rev. Lett. **81**, 3227 (1998).
- ⁷ A. Ino, C. Kim, M. Nakamura, T. Yoshida, T. Mizokawa, Z.-X. Shen, A. Fujimori, T. Kakeshita, H. Eisaki, and S. Uchida, cond-mat/9902048.
- ⁸ B.O. Wells, Z.-X. Shen, A. Matsuura, D.M. King, M.A. Kastner, M. Greven, and R.J. Birgeneau, Phys. Rev. Lett. **74**, 964 (1995).
- ⁹ L.N. Bulaevskii, E.L. Nagaev, and D.L. Khomskii, Sov. Phys. JETP **27F**, 836 (1968).
- ¹⁰ S. Trugman, Phys. Rev. B **37**, 1597 (1988); *ibid.*, **41**, 892 (1990).
- ¹¹ E. Dagotto, Rev. Mod. Phys. **66**, 763 (1994).
- ¹² A. Nazarenko, K. J. E. Vos, S. Haas, E. Dagotto, and R. J. Gooding, Phys. Rev. B. **51**, 8676 (1995).
- ¹³ P. W. Leung, B. O. Wells, and R. J. Gooding, Phys. Rev. B **56**, 6320 (1997).
- ¹⁴ R. Eder, Y. Ohta, and G. A. Sawatzky, Phys. Rev. B, **55**, 3414 (1997).
- ¹⁵ V. I. Belinicher, A. L. Chernyshev, V. A. Shubin, Phys. Rev. B **53**, 335 (1996).
- ¹⁶ F. Lema, A. A. Aligia, Phys. Rev. B **55**, 14092 (1997).
- ¹⁷ J.R.Schrieffer, X.G.Wen, and S.C. Zhang, Phys. Rev. B **39**, 11663 (1989).
- ¹⁸ R. Eder und K. W. Becker, Z. Phys. B. **78**, 219 (1990).
- ¹⁹ R. Eder und K. W. Becker, Phys. Rev. B **44**, 6982 (1991); O. P. Sushkov, G. A. Sawatzky, R. Eder and H. Eskes, Phys. Rev. B. **56**, 11769 (1997).
- ²⁰ H. Eskes and R. Eder, Phys. Rev. B. **54**, 14226 (1996).
- ²¹ J. M. Eroles, C. D. Batista, A. A. Aligia, Phys. Rev. B **59**, 14 092 (1999).
- ²² A. Bianconi A, N.L. Saini, A. Lanzara, M. Missori, T. Rossetti, H. Oyanagi, H. Yamaguchi, K. Oka, T. Ito, Phys. Rev. Lett. **76**, 3412 (1996).
- ²³ R. Eder and P. Wróbel, Phys. Rev. B **47**, 6010 (1993).
- ²⁴ R. Eder, P. Wróbel, and Y. Ohta, Phys. Rev. B **54**, R11034 (1996).
- ²⁵ R. R. Bartkowski, Phys. Rev. B **5**, 4436 (1972).
- ²⁶ K. W. Becker and P. Fulde, J. Chem. Phys. **91**, 4223 (1989).
- ²⁷ K. W. Becker and W. Brenig, Z. Phys. B **79**, 195 (1990).

FIG. 1. Stripe structure for 12.5% of doping which have been applied = in the calculation of the hole dispersion. Solid circles depict immobile holes within the stripes, arrows represent spins in antiphase AF domains that separate the stripes.

FIG. 2. Some processes related to direct hopping to next nearest neighbors.

FIG. 3. A process related to direct hopping to third nearest neighbors.

FIG. 4. A processes related to the exchange term.

¹ J.M. Tranquada *et al*, Nature **375**, 561 (1995); Phys. Rev. B **54**, 74898 (1996).

² J. Zaanen and O. Gunnarson, Phys. Rev. B **40**, 7391 (1989).

³ D. Poilblanc and T. M. Rice, Phys. Rev. B **39**, 9749 (1989).

⁴ P. Prelovshchek and X. Zotos, Phys. Rev. B **47**, 5984 (1993).

⁵ R. Eder, Y. C. Chen, H. Q. Lin, Y. Ohta, C. T. Shih, and T. K. Lee, Phys. Rev. B. **55**, 12313 (1997).

FIG. 5. Structure applied in the calculation for the case of 1 hole per 12 sites.

FIG. 6. Spectral functions in the $(0, 0) \rightarrow (\pi, 0)$ direction for points separated by an equal distance.

FIG. 7. Spectral functions in the $(0, 0) \rightarrow (0, \pi)$ direction for points separated by an equal distance.

FIG. 8. Spectral functions in the $(\pi, 0) \rightarrow (\pi, \pi)$ direction for points separated by an equal distance.

FIG. 9. Spectral functions in the direction $(0, \pi) \rightarrow (\pi, \pi)$ for points separated by an = equal distance.

FIG. 10. Spectral functions in the direction $(0, 0) \rightarrow (\pi, \pi)$ for points separated by an = equal distance.

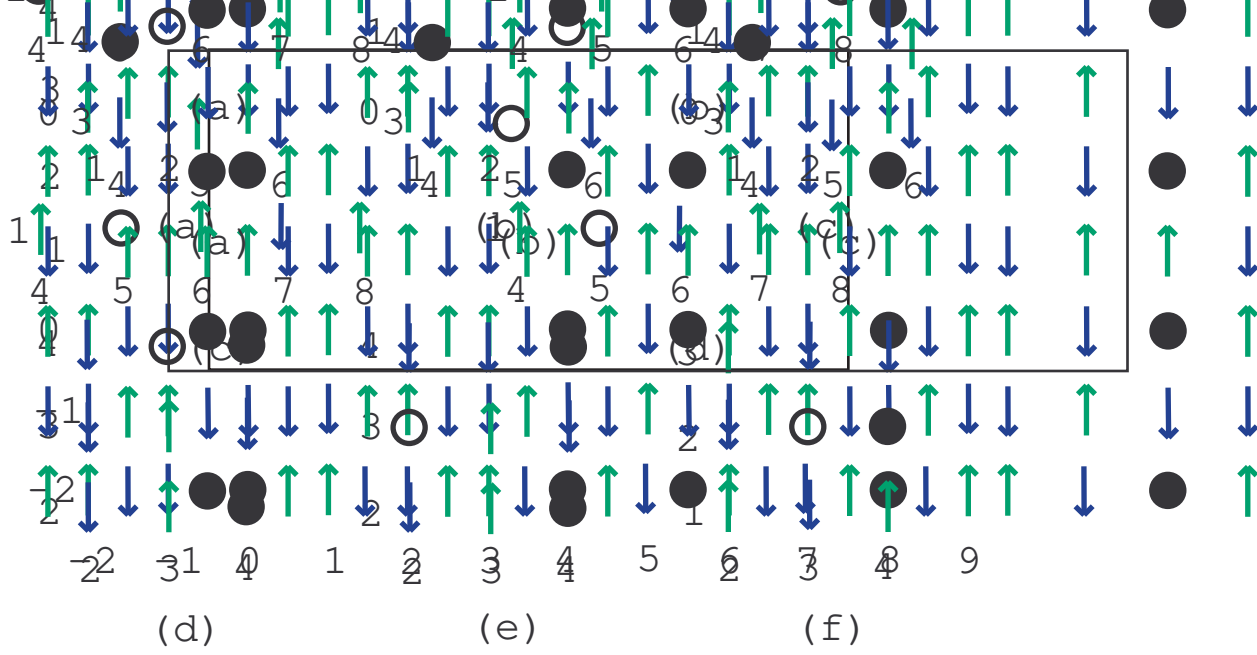
FIG. 11. Quantum mechanical probability w that an additional hole is in the polaron state at a particular site in the stripe structure for a wave function related to a dominant peak in the spectral function at the energy about $-1.60t$ for $\mathbf{p} = 3D(\pi, 0)$.

FIG. 12. Quantum mechanical probability w that an additional hole is in the polaron state at the site n in the stripe structure for a wave function related to a recognizable peak in the spectral function at the energy about $-2.23t$ for $\mathbf{p} = 3D(\pi, 0)$. The hole stripes are in the 0^{th} and 4^{th} column.

FIG. 13. Quantum mechanical probability w that an additional hole is in the polaron state at a particular site in the stripe structure for a wave function related to a dominant peak in the spectral function at the energy about $-1.63t$ for $\mathbf{p} = 3D(0, \pi)$.

FIG. 14. Spectral functions in the $(0, 0) \rightarrow (\pi, 0)$ direction for points separated by an equal distance. Calculation was performed for the structure depicted in Fig. 5.

FIG. 15. Spectral functions in the direction $(0, 0) \rightarrow (\pi, \pi)$ for points separated by an equal distance. Calculation was performed for the structure depicted in Fig. 5.



This figure "fig6.gif" is available in "gif" format from:

<http://arxiv.org/ps/cond-mat/0006022v1>

This figure "fig7.gif" is available in "gif" format from:

<http://arxiv.org/ps/cond-mat/0006022v1>

This figure "fig8.gif" is available in "gif" format from:

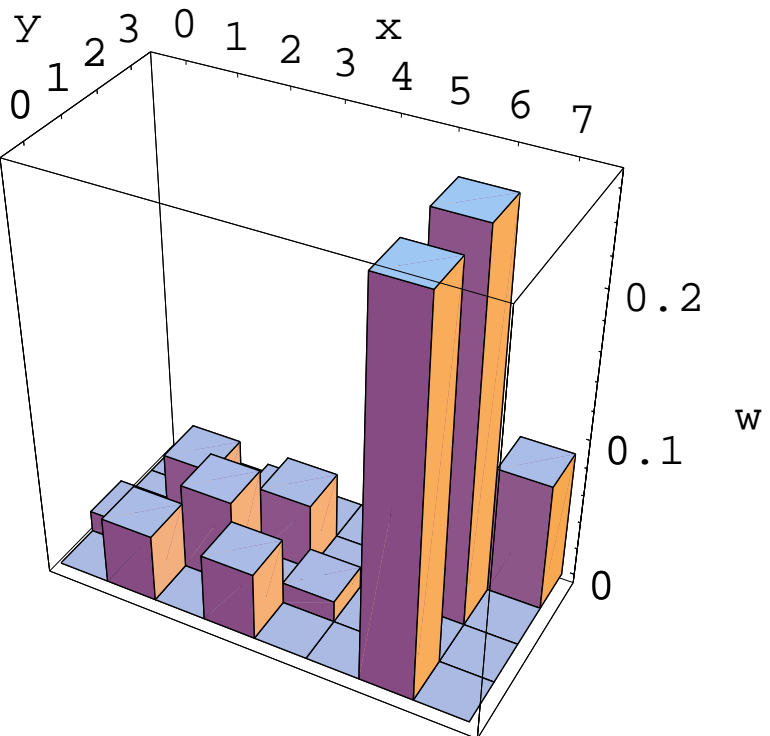
<http://arxiv.org/ps/cond-mat/0006022v1>

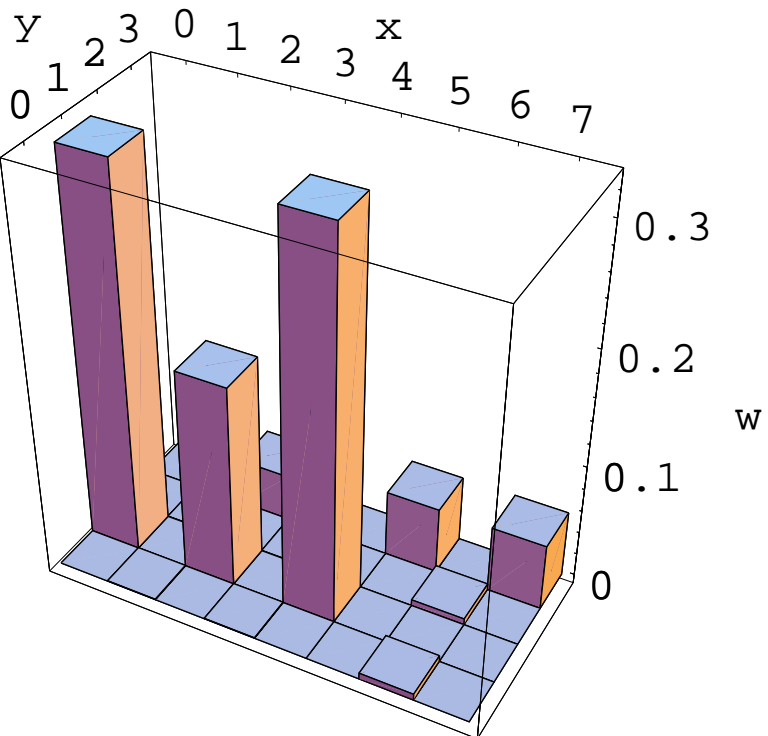
This figure "fig9.gif" is available in "gif" format from:

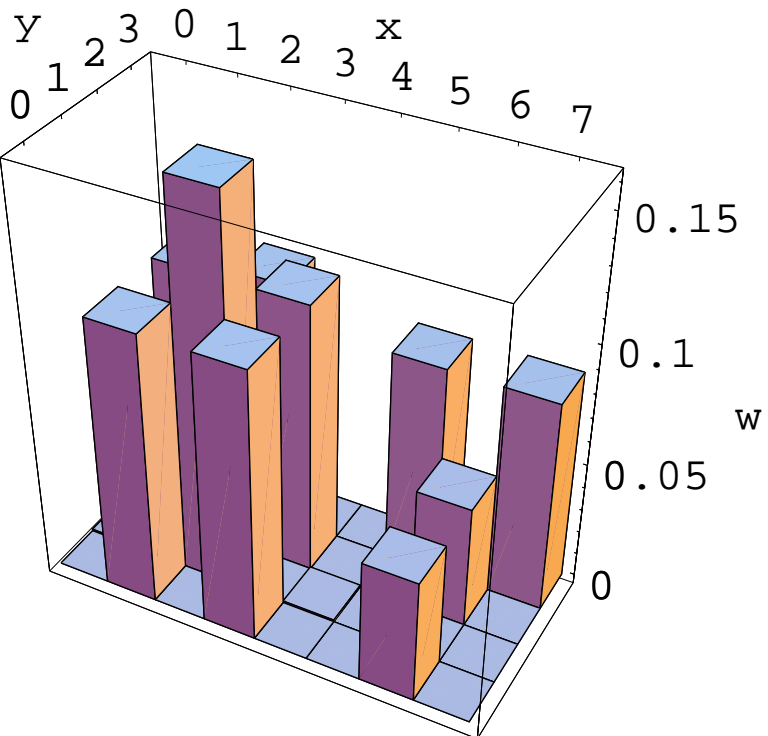
<http://arxiv.org/ps/cond-mat/0006022v1>

This figure "fig10.gif" is available in "gif" format from:

<http://arxiv.org/ps/cond-mat/0006022v1>







This figure "fig14.gif" is available in "gif" format from:

<http://arxiv.org/ps/cond-mat/0006022v1>

This figure "fig15.gif" is available in "gif" format from:

<http://arxiv.org/ps/cond-mat/0006022v1>